

Solvent Effect on Electronegativity, Hardness, Condensed Fukui Functions, and Softness, in a Large Series of Diatomic and Small Polyatomic Molecules: Use of the EFP Model

Bennasser Safi,[†] Robert Balawender,^{†,‡} and Paul Geerlings^{*,†}

Eenheid Algemene Chemie (ALGC), Faculteit Wetenschappen, Vrije Universiteit Brussel, Pleinlaan 2, B-1050 Brussels, Belgium, and Institute of Physical Chemistry, Polish Academy of Sciences, Kasprzaka 44/52, PL-01-224 Warsaw, Poland

Received: July 11, 2001; In Final Form: October 8, 2001

The effect of solvent on the electronegativity, hardness, and condensed Fukui function, and atomic softness for a set of diatomic and small polyatomic molecules and ions has been studied using the effective fragment potential (EFP) model. The binding function was used for monitoring the solvation of the molecule. We do not observe a decrease in the HOMO–LUMO gap in the solvent. All anions show a significant change in the chemical potential. Both HOMO and LUMO energy levels decrease in the solvent phase as compared to the gas phase. For the major part of the acids, the increase in the LUMO orbital energy is larger than in the HOMO orbital energy. For the group of salts, we observe an increase in the LUMO energy level and a similar decrease in the HOMO energy level, resulting in a small change in the chemical potential. The importance of the change in the wave function upon solvation was shown through an analysis of the relaxation part in the hardness and condensed Fukui function. Very close values found for the same ions in molecules such as LiH, LiF, NaH, NaF, and LiF indicate that in these cases very good separated ion pairs are present.

I. Introduction

In recent years, density functional theory^{1,2} revolutionized quantum chemistry. Concentrating on electron density as the fundamental property describing the ground state of an atomic or molecular system leads to better quality/cost ratios when evaluating molecular properties. On the other hand, it opened, under the impetus of Parr, the way to sharp definitions of chemical concepts, already in use for many years, thus affording their calculation and systematic use in discussing chemical reactivity. Global reactivity descriptors of this type are electronegativity (χ), chemical potential (μ),³ global hardness (η),⁴ and global softness (S), examples of local reactivity descriptors being hardness and softness kernel,⁵ local softness [$s(\mathbf{r})$],⁶ and Fukui function [$f(\mathbf{r})$].⁷ The hard and soft acids and bases principle,⁸ the electronegativity equalization principle,⁹ and the maximum hardness principle¹⁰ have been used in quantitative structure–reactivity relationships. While the global hardness has been found to be reliable in generating intermolecular reactivity trends, $s(\mathbf{r})$ and $f(\mathbf{r})$ are increasingly used as reliable intermolecular (site selective) reactivity descriptors.

In the past, the concepts of hardness and softness were used, together with their local counterparts, in an abundance of reactivity studies, in our group among others.^{11–14} However, almost all of the calculations of these properties were performed in the gas phase. Recently, the concepts of functional group electronegativity, hardness, and softness were calculated using a continuum model; the values that were obtained were then used in the study of the acidity of alkyl-substituted alcohols and amines.^{15,16} Contreras et al. have also studied relations

between solvation energy, chemical potential, hardness, and linear response functions,^{17–19} and the effect of solvent on the reaction of enolate ions with methyl chloride using a pair site reactivity model derived from a second-order static density response function.²⁰

In a previous paper,²¹ we made an attempt to incorporate direct solute–solvent interaction schemes, avoiding however a complete supermolecule-type approach, using Gordon's effective fragment potential (EFP) approach.^{22,23} In this method, one typically divides the total system into two parts, an ab initio or active region and a fragment region. Then the fragment–fragment and/or fragment–ab initio interactions are calculated using a simplified methodology (see section II.2). This model has been applied in studies on ribonuclease,²⁴ small water clusters,²⁵ formamide,^{26,27} glutamic acid,²⁸ and water–sodium chloride clusters.²⁹ A combined EPF/Onsager model (discrete/continuum model) recently has been used for calculation of the relative stabilities of the neutral and zwitterionic forms of glycine.³⁰

In our earlier contribution,²¹ the EFP methodology was combined with this approach to study the solvent effect on the global and atomic DFT-based reactivity descriptors in the case of ammonia. A saturation effect was observed where the target molecule was surrounded by more than 16 fragment water molecules. In this paper, the solvent effect on these reactivity descriptors is discussed for a large series of neutral and charged molecules containing first- and second-row elements (LiF, LiH, NaF, NaH, HF, HCl, HCN, BeH₂, BH₃, CO, H₂CO, NH₃, H₂O, PH₃, H₂S, CH₃⁺, NH₄⁺, CN[−], NH₂[−], OH[−], SH[−], Br[−], Cl[−], and F[−]) considering water as a solvent. The DFT-based reactivity descriptors are calculated from coupled perturbed Hartree–Fock (CPHF) equations.^{31,32} The importance of changes in the geometry of the molecules is discussed in terms of the binding function, introduced by Wang and Peng³³ and recently successfully used by us in a study on the Jahn–Teller effect.³⁴

* To whom correspondence should be addressed. E-mail: pgeerlin@vub.ac.be. Telephone: 00 32 2 629 33 14. Fax: 00 32 2 629 33 17.

[†] Vrije Universiteit Brussel.

[‡] Polish Academy of Sciences.

The paper is organized as follows. In section II, the three aspects of the theoretical foundations are discussed: definition and working equations for DFT reactivity descriptors and their evaluation via the coupled perturbed Hartree–Fock formalism (II.1), the incorporation of the solvent effect via the EFP method (II.2), and the evaluation of the binding function (II.3). After a section on computational details (section III), Results and Discussion are presented in section IV.

II. Theory

II.1. DFT Reactivity Descriptors in the Gas Phase: The CPHF Approach. Global and local DFT reactivity descriptors such as chemical potential (μ) [negative of the electronegativity (χ)], hardness (η), or Fukui function [$f(\mathbf{r})$]

$$\chi = -\mu = -\left(\frac{\partial E}{\partial N}\right)_{v(\mathbf{r})} \quad (1)$$

$$\eta = \frac{1}{2}\left(\frac{\partial^2 E}{\partial N^2}\right)_{v(\mathbf{r})} = \frac{1}{2}\left(\frac{\partial \mu}{\partial N}\right)_{v(\mathbf{r})} \quad (2)$$

$$f(\mathbf{r}) = \left[\frac{\partial \rho(\mathbf{r})}{\partial N}\right]_{v(\mathbf{r})} \quad (3)$$

are typically derivatives with respect to the total number of electrons, N , at a constant external potential, $v(\mathbf{r})$ (“frozen” geometry of the molecule), $[(\partial)/(\partial N)]_{v(\mathbf{r})}$.¹¹ The derivatives at some integral value N_0 will in general have different values at the right-hand side ($N_0 + \delta$, electron inflow, chemical reduction) and left-hand side ($N_0 - \delta$, electron outflow, chemical oxidation). Their average indicates reactivity toward a radical reagent. The coupled perturbed Hartree–Fock approach, presented in ref 31, offers an interesting alternative to the “popular” finite difference approach in which the reactivity parameters are obtained by calculating the quantities to be differentiated numerically for different but necessarily integer N values.

From the chain rule, we have

$$\left(\frac{\partial}{\partial N}\right)_{v(\mathbf{r})} = \left(\frac{\partial}{\partial \mathbf{n}}\right)_{v(\mathbf{r}), \mathbf{C}} \left(\frac{\partial \mathbf{n}}{\partial N}\right)_{v(\mathbf{r})} + \left(\frac{\partial}{\partial \mathbf{C}}\right)_{v(\mathbf{r}), \mathbf{n}} \left(\frac{\partial \mathbf{C}}{\partial N}\right)_{v(\mathbf{r})} \quad (4)$$

where the \mathbf{n} diagonal matrix contains the MO occupations (two for an occupied MO and 0 for a virtual MO) and \mathbf{C} is the wave function coefficients matrix. For canonical orbitals and with conditions under which only the highest occupied (HO) and lowest unoccupied (LU) MO are involved during electron displacements, the \mathbf{f} matrix defined as $\mathbf{f} = (\partial \mathbf{n} / \partial N)_{v(\mathbf{r})}$ has the form

$$f_i^\pm = \begin{cases} 1 & \text{for } i = \text{LUMO/HOMO} \\ 0 & \text{for } i \neq \text{LUMO/HOMO} \end{cases} \quad (5)$$

Within the CPHF approach, and concentrating on the restricted Hartree–Fock (RHF) theory, we may expand the derivative of the μ th coefficient of the i th MO with respect to N in the basis of the unperturbed MOs:^{31,32}

$$\left(\frac{\partial c_{\mu i}}{\partial N}\right)_{v(\mathbf{r})} = \sum_k^{\text{MO}} c_{\mu k} U_{ki} \text{ or } \left(\frac{\partial \mathbf{C}}{\partial N}\right)_{v(\mathbf{r})} = \mathbf{C}\mathbf{U} \quad (6)$$

where the \mathbf{U} matrix element is equal to

$$U_{ij}^\pm = \sum_k^{\text{vir}} \sum_l^{\text{occ}} A_{ij,kl}^{-1} \left[(kl|\text{FMO}, \text{FMO}) - \frac{1}{2}(k, \text{FMO}|l, \text{FMO}) \right] \quad (7)$$

where i is the virtual MO, j is the occupied orbital, FMO is the

frontier molecular orbital, and $ij|kl$ stands for a two-electron repulsion integral in the MO basis.

The symmetrical \mathbf{A} matrix is defined as

$$A_{ij,kl} = \delta_{ij,kl}(e_i - e_j) - 4(ij|kl) + (ik|jl) + (il|jk) \quad (8)$$

Electronegativity, the first derivative of the energy with respect to n , can be written as

$$\mu^\pm = \left(\frac{\partial E}{\partial N}\right)_{v(\mathbf{r})}^\pm = e_{\text{LUMO/HOMO}} \quad (9)$$

where e_{HOMO} and e_{LUMO} are frontier orbital energies. The global hardness, the second derivative of the energy with respect to N , is thereby expressed as

$$\eta = \frac{1}{2}\left(\frac{\partial \mu}{\partial N}\right)_{v(\mathbf{r})} = \frac{1}{4}J_{\text{FMO}} + \sum_i^{\text{vir}} \sum_j^{\text{occ}} U_{ij} [2(i,j|\text{FMO}, \text{FMO}) - (i, \text{FMO}|j, \text{FMO})] \quad (10)$$

where $J_{\text{FMO}} [= (\text{FMO}, \text{FMO}|\text{FMO}, \text{FMO})]$ is the Coulomb integral for the frontier orbital (FMO). The first term represents the contribution from the change of the molecular occupation at frozen wave functions, $\eta^{\text{f}\pm}$, and the second represents the contribution from relaxation of the wave function, $\eta^{\text{U}\pm}$.

The condensed version of the local Fukui function $\{f(\mathbf{r}) = [\partial \rho(\mathbf{r}) / \partial N]_{v(\mathbf{r})}\}$, for atom A, given by the derivative of the atomic population n_A , can be written as

$$\left(\frac{\partial n_A}{\partial N}\right)_{v(\mathbf{r})}^\pm = f_A^{\text{f}\pm} + f_A^{\text{U}\pm} = f_A^\pm \quad (11)$$

where

$$f_A^{\text{f}\pm} = \sum_{\mu \in A}^{\text{AO}} \sum_v^{\text{AO}} c_{\text{FMO}\mu} c_{\text{FMO}v} S_{\mu v}, \text{ and} \\ f_A^{\text{U}\pm} = 2 \sum_k^{\text{vir}} \sum_i^{\text{occ}} U_{ki}^\alpha \sum_{\mu \in A}^{\text{AO}} \sum_v^{\text{AO}} (c_{k\mu} c_{iv} + c_{i\mu} c_{kv}) S_{\mu v}.$$

$S_{\mu v}$ represents the elements of the overlap matrix. f_A^{f} accounts for the effect of changing only MO occupations. The second term f_A^{U} represents the MO relaxation contribution for frozen MO occupations. The contributions from the occupied–occupied and virtual–virtual orbital interactions vanish due to the antisymmetric property of the \mathbf{U} matrix ($\mathbf{U}^T = -\mathbf{U}$).

Another local property, local softness $\{s(\mathbf{r}) = [\partial N / \delta \rho(\mathbf{r})]_{v(\mathbf{r})} = f(\mathbf{r})S\}$, where $S (= 1/2\eta)$ is the global softness, in its condensed version, atomic softness, can be calculated as

$$s_A^\pm = f_A^\pm S^\pm \quad (12)$$

Hereby, however, we have to differentiate between the average value of the softness in the form $\bar{s}_A = 1/2(s_A^+ + s_A^-)$ and as $s_A^0 = f_A^0 S^0$ [their difference being $1/4(f_A^- S^+ + f_A^+ S^-)$].

The set of equations presented above permits evaluation of the DFT-based reactivity descriptors within the CPHF scheme. Note that the use of a non-DFT calculation technique does not contradict the use of DFT-based reactivity descriptors.¹¹

II.2. Inclusion of the Solvent Effect: The Effective Fragment Potential Method. In general, the EFP model treats each solvent molecule explicitly, by adding one-electron terms directly to the ab initio Hamiltonian:

$$H_{\text{TOT}} = H_{\text{AR}} + V \quad (13)$$

where H_{AR} is the ab initio Hamiltonian describing the “active region” of the system (solute and any solvent molecules that directly participate in the bond making or breaking process).

$$V = V^{\text{elec}} + V^{\text{pol}} + V^{\text{rep}} \quad (14)$$

The three one-electron terms in V , representing the potential due to the solvent (fragment) molecules, correspond to electrostatic, polarization, and exchange repulsion/charge transfer interactions between the solvent molecules and the electrons and nuclei in the active region, as well as solvent–solvent interactions. There are no exchange repulsion/charge transfer terms in the nuclear–solvent interaction. The solute (including the desired number of solvent molecules) is treated explicitly with the ab initio wave function technique of choice, while the solvent is represented by effective fragments. To incorporate the EFP model into our calculation, the Fock matrix is modified to include the contribution from effective fragments by introduction of the \mathbf{V} matrix

$$\mathbf{F} = \mathbf{H} + \mathbf{G} + \mathbf{V} \quad (15)$$

where \mathbf{H} and \mathbf{G} stand for one- and two-electron integrals matrix in the MO basis, respectively.

These elements of the \mathbf{V} matrix contain the operator for the interaction between the fragment and the electron density matrix (\mathbf{V}^{ef} operator for the interaction fragment electron density)

$$\mathbf{V} = \mathbf{C}^T \mathbf{V}^{\text{ef}} \mathbf{C} \quad (16)$$

The additional term in the Fock matrix changes the geometry of the solute which affects the atomic orbital integrals and the wave function coefficients. There is also an additional contribution from the interaction between solvent (in the case of water) fragments and the solute molecule electron density. The chemical potential, eq 1, is then written as

$$\mu^{\pm} = \epsilon_{\text{FMO}}^{\text{sol}} = H_{\text{FMO}}^{\text{sol}} + G_{\text{FMO}}^{\text{sol}} + V_{\text{FMO}}^{\text{sol}} \quad (17)$$

Differences in the hardness value find their origin in the change in the AO integrals, the \mathbf{C} and \mathbf{U} matrices. But there is no direct contribution from the \mathbf{V} matrix, as we have in the chemical potential case. The Fukui function in the solvent changes as compared to the gas phase because of differences in the \mathbf{C} and \mathbf{U} matrices. There is also a contribution from the change in the geometry, which is expressed directly in the difference of the overlap matrix in the solvent versus the gas phase.

II.3. Binding Function. We used the binding function as an index of the change in the molecular geometry due to solvation. The binding function F_B is defined as the virial of the forces necessary to hold all the nuclei in the molecule fixed (M is the number of atoms in the molecule).³³

$$F_B = \sum_{\alpha=1}^M \mathbf{R}_{\alpha} \nabla_{\alpha} W = - \sum_{\alpha=1}^M \mathbf{R}_{\alpha} \mathbf{F}_{\alpha} \quad (18)$$

Here \mathbf{R}_{α} denotes the position of nucleus α and the summation runs over all nuclei. A positive value of the binding function (the virial) means that the forces on the nuclei are acting “into the molecule” [$\cos(\angle(\mathbf{R}_{\alpha}, \mathbf{F}_{\alpha}))$ is negative], resulting in a binding effect; if the binding function is negative, forces are “acting out” of the system [$\cos(\angle(\mathbf{R}_{\alpha}, \mathbf{F}_{\alpha}))$ is positive] and try to enlarge its structure, resulting in an antibinding effect. Of course, in the equilibrium geometry, the binding function is equal to zero. In a previous paper,³² we studied the evolution of F_B with a changing number of electrons. In analogy, we now study the

change in F_B , ΔF_B , when the molecular geometry changes when passing from the gas phase to aqueous solution. But we take F_B as the value of the binding function of the molecule with the geometry it adopts in solution and compare it to the gas phase (after optimization in the solvent; we remove all molecules of water and then calculate the binding function).

III. Computational Details

For the series of molecules mentioned in the Introduction, the values of the chemical potential, the HOMO–LUMO energy gap, the global hardness, and the atomic properties such as the Mulliken population and the atomic softness were calculated both in the gas phase and in aqueous solution. On the basis of our results in ref 21 (the saturation point for solvation of ammonia was located around a cluster with 16 water molecules), the latter situation was treated via the EPF model using a surrounding of 30 water molecules. The EFP model is used in a rigid body approximation: the internal coordinates of the solvent molecule fragments (H_2O) are fixed (O–H bond length of 0.944 Å, H–O–H angle of 106.7°), whereas all fragment positions relative to the solute or each other are fully optimized. For each species, we have generated 50 structures using a random number generator procedure described in ref 18 and starting from 6-31G*-optimized gas phase structures. For all structures, we have performed a two-step geometry optimization using the GAMESS program with option POSITION=EFOPT in the \$EFRAG mode and with the gradient convergence tolerance equal to 10^{-7} Hartree/Bohr.³⁵ We then have taken the ~ 10 lowest-energy structures for which we have performed full geometry optimizations at the restricted Hartree–Fock level using the 6-31G* basis. Finally, we have calculated both global properties (chemical potential and hardness) and atomic indices (condensed Fukui function and atomic softness) in the gas phase and in the solvent, using the coupled perturbed HF equations, and the change in binding function.^{31,32}

As the number of local minima on the potential energy surface rapidly increases with an increase of the number of water fragments, we decided to use only an average value of the reactivity indices obtained for a given molecule surrounded by 30 water molecules.

IV. Results and Discussion

IV.1. Effect of Solvent on Global Properties Such as Electronic Chemical Potential, Electronegativity, and Hardness. The solvation of a protic acid (e.g., HCl, HF, ...) in water may be monitored by detecting the formation of the hydronium ion H_3O^+ , but for salts such as LiF and NaF, such a simple species is not available. Another way is to monitor the change in the molecular structure using the binding function. The values of the binding function and the solvation energy for the complete series of ions and molecules are listed in Table 1. Values of the binding function for LiF, LiH, NaF, NaH, and BeH_2 are 1 order of magnitude larger than for the other species. The positive value indicates that the solvent “enlarges” the molecule. The geometries of LiH, LiF, NaH, and NaF change considerably in the solvent. Equilibrium distances increase from 1.55 to 1.96 Å (LiH), from 1.56 to 1.70 Å (LiF), from 1.91 to 2.44 Å (NaH), and from 1.96 to 2.10 Å (NaF), indicating (partial) dissociation into solvent-separated ion pairs with the solvation energy equal to approximately -330 kcal/mol. For BeH_2 , the large value is produced by passing from the linear to the bent form (the H–Be–H angle varies from 180° to 120°). For the rest of the molecules, we did not observe significant changes in geometry. We can explain this as an effect of the method that was used.

TABLE 1: Binding Function (in arbitrary units), Solvation Energies (in kilocalories per mole), Average Chemical Potential Values (μ), Half of the HOMO–LUMO Energy Gap ($\Delta_{HL}/2$), and Their Differences between the Solvent and Gas Phase [$\Delta\mu$ and $\Delta(\Delta_{HL}/2)$] (all values in electronvolts)

molecule	binding function	solvation energy	μ (in gas)	$\Delta\mu$	$\Delta_{HL}/2$ (in gas)	$\Delta(\Delta_{HL}/2)$
LiF	0.125	-328	-6.150	1.252	6.313	2.558
LiH	0.104	-331	-3.946	1.034	4.163	2.639
NaF	0.121	-328	-5.551	0.517	5.415	2.939
NaH	0.111	-323	-3.701	0.435	3.701	2.721
FH	0.043	-280	-5.578	1.905	11.538	1.442
HCl	0.010	-274	-4.163	1.088	8.789	0.789
HCN	-0.006	-278	-3.674	-0.354	9.361	0.218
BeH ₂	0.129	-296	-4.816	2.721	7.293	0.925
BH ₃	-0.002	-268	-5.551	1.061	7.973	0.517
CO	0.000	-272	-5.143	0.163	9.714	0.054
H ₂ CO	0.020	-274	-3.946	0.190	7.918	0.163
NH ₃	0.003	-277	-2.667	-0.054	8.735	0.844
H ₂ O	0.026	-285	-3.891	0.844	9.687	1.034
PH ₃	-0.021	-272	-2.884	-0.027	7.510	0.136
H ₂ S	-0.008	-273	-2.884	0.163	7.565	0.299
CH ₃ ⁺	-0.051	-339	-16.844	8.653	9.225	0.680
NH ₄ ⁺	-0.007	-341	-14.612	4.626	12.844	0.408
CN ⁻	-0.016	-331	5.088	-5.578	9.197	0.109
NH ₂ ⁻	-0.052	-363	7.157	-5.905	7.102	1.279
OH ⁻	-0.023	-370	7.157	-6.667	8.163	1.469
SH ⁻	-0.015	-328	5.252	-4.898	7.157	0.544
Br ⁻	0	-329	8.163	-5.225	10.966	0.027
Cl ⁻	0	-331	9.469	-5.878	12.844	0.000
F ⁻	0	-362	20.000	-8.980	22.095	0.109

In the EFP model, we do not account for a possible flow of electrons between the solvent and the solute; if the electronegativity of the atoms in the solute is sufficiently high, they can only form a hydrogen bond with water fragments. For protic acids, such as HCl, HF, and HCN, the hydronium ion H₃O⁺ is formed during solvation, but when the internal coordinates of the water molecule are frozen, no such simple species is available. This result can be interpreted via the binding function values given in Table 1 which are on average 1 order of magnitude larger in the aforementioned cases than for nondissociating species. The positive value indicates that upon relaxing the interatomic distance tends to decrease.

Hydrogen bonding plays a crucial role in the interactions between a neutral molecule or ion and a solvent like H₂O. Due to the small size of the atom, small monatomic anions such as F⁻ and Cl⁻ are more solvated than the larger ones, e.g., Br⁻. This is also the reason the solvation energy of the ions increases in the following order: F⁻ > Cl⁻ > Br⁻ and OH⁻ > NH₂⁻ > SH⁻. It is pleasing to see that the solvation energy sequence (OH⁻ ≥ F⁻ > Cl⁻ ≥ Br⁻) parallels experimental data.^{36,37} According to those sequences, the solvation energies follow the same sequence as the hardness (see the values given in Table 1): $\eta(\text{F}^-) > \eta(\text{Cl}^-) > \eta(\text{Br}^-)$ and $\eta(\text{OH}^-) > \eta(\text{NH}_2^-) > \eta(\text{SH}^-)$. From these results, we can conclude that the larger the solvation energy, the more the solute softness is reduced. This is in agreement with the experimental results³⁸ predicting that a solvated species become less polarizable in the presence of a polar medium.

Figure 1 presents the change in the chemical potential and in Δ_{HL} ($\epsilon_{\text{LUMO}} - \epsilon_{\text{HOMO}}$) upon solvation. For no species do we observe a decrease in the gap between the HOMO and the LUMO. These results are in agreement with the conclusion reported by Pearson on the basis of effective ionization potentials and electron affinities in solution from redox potentials.^{38–40} All anions exhibit a significant change in chemical potential. While the energy of the HOMO is decreasing, the change in the energy LUMO orbital is also negative. As a result, the anions

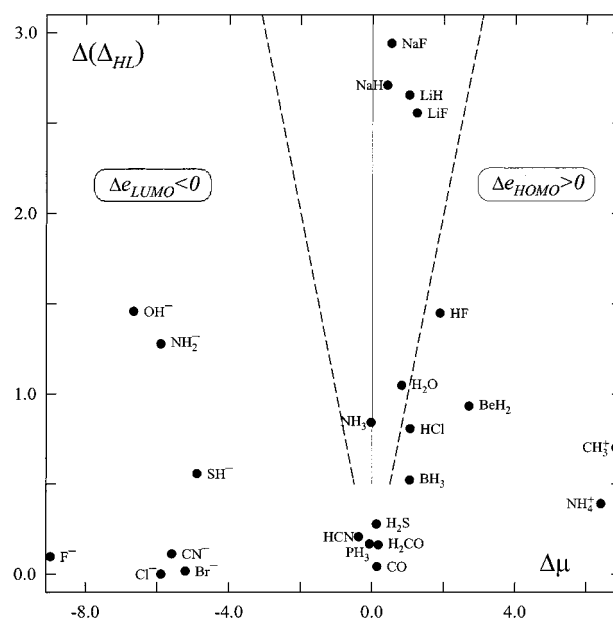


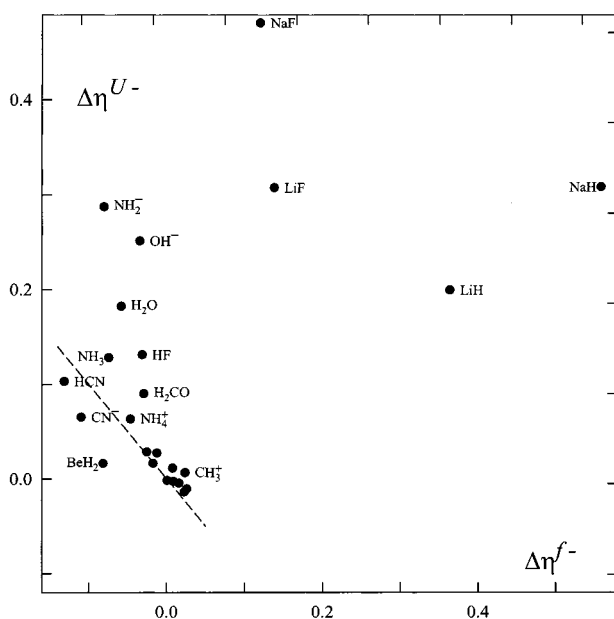
Figure 1. Change in the electronic chemical potential, $\Delta\mu$, vs the change in the HOMO–LUMO energy gap, $\Delta(\Delta_{HL}/2)$, upon solvation. Points at the left on the first dotted line have negative values for the change in the LUMO energy ($\Delta\epsilon_{\text{LUMO}} < 0$), and points to the right of the second dotted line have positive values for the change in the HOMO energy ($\Delta\epsilon_{\text{HOMO}} > 0$) (all values in electronvolts).

are stabilized and the solvent reduces its electron donor capacity, as compared to that in the gas phase. For the halide anions and CN⁻, the energy shift of the HOMO is close to the change in energy of the LUMO and Δ_{HL} does not change appreciably. For the major part of the acids, we observe an increase in the energies of both frontier orbitals, the increase for the LUMO turning out to be larger than that for the HOMO. For the two cations in our series, we observe a strong influence of the solvent on the electronic chemical potential, which increases by more than 4 eV. This indicates that the cations become weak electron acceptors in water. These results are in agreement with the conclusion very recently reported by Pérez, Toro-Labbé, and Contreras (after this work had been completed) in a continuum model study on solvent effects on electrophilicity.⁴¹ Increasing the HOMO energy for this molecule may be interpreted as an increasing donor electron ability. In conclusion, the solvent stabilizes both cations and anions, making the cations poorer electron acceptors and the anions poorer electron donors in solution, as compared to the gas phase. For the group of neutral molecules, which manifest significant changes in the geometry, we observe an energy gap. LiF, LiH, NaH, and NaF are examples of Lewis acid–base compounds. Water is a hard solvent and can further harden hard molecules, in reactions with hard acids (Li⁺ and Na⁺) playing the role of a hard base and with F⁻ as a hard acid.⁴² For this group of neutral systems, we observe an increase in the LUMO energy level and a similar decrease in the HOMO energy level, resulting in a small change in the chemical potential, again in agreement with Toro-Labbé’s prediction.⁴¹

The hardness calculated via the coupled perturbed HF equations can be divided into two parts: a “rigid” part corresponding to “frozen” wave function coefficients allowing only changes in the occupation of the MOs, η^f , and a part representing contributions from changes in the wave function coefficients, the relaxation part, η^U . The hardness values are summarized in Table 2. The changes in both parts are shown in Figures 2 and 3. Points situated above the dotted line indicate

TABLE 2: Electrophilic Hardness (η^-), Nucleophilic Hardness (η^+), Their Differences between the Solvent and Gas Phase ($\Delta\eta^-$ and $\Delta\eta^+$), and the Difference between the Components of the Hardness Calculated in Solvent and in the Gas Phase (see the text; all values in electronvolts)

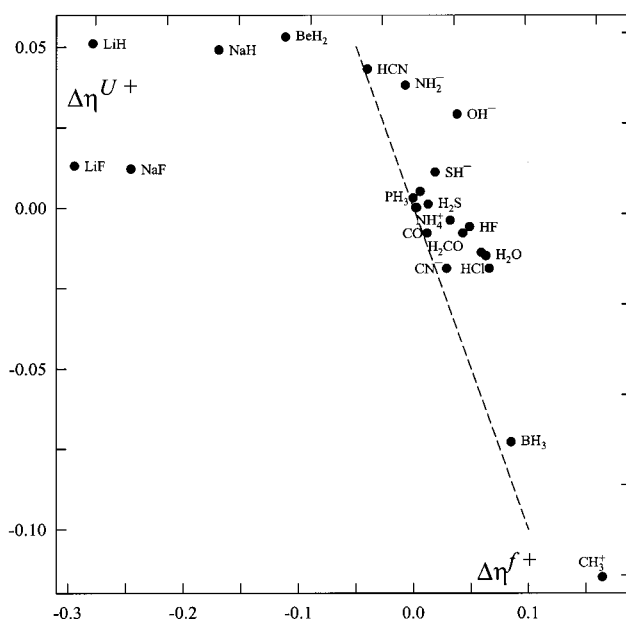
molecule	$\Delta\eta^{f-}$	$\Delta\eta^{U-}$	η^- (in gas)	$\Delta\eta^-$	$\Delta\eta^{f+}$	$\Delta\eta^{U+}$	η^+ (in gas)	$\Delta\eta^+$
LiF	0.138	0.307	2.650	0.447	-0.294	0.013	1.513	-0.283
LiH	0.364	0.199	2.642	0.561	-0.278	0.051	1.478	-0.229
NaF	0.120	0.481	2.531	0.598	-0.245	0.012	1.263	-0.234
NaH	0.559	0.308	2.357	0.865	-0.169	0.049	1.211	-0.120
FH	-0.031	0.131	3.461	0.101	0.049	-0.006	2.588	0.043
HCl	-0.012	0.027	2.498	0.016	0.066	-0.019	2.158	0.046
HCN	-0.131	0.103	2.694	-0.027	-0.040	0.043	2.169	0.002
BeH ₂	-0.081	0.016	2.514	-0.065	-0.111	0.053	1.769	-0.060
BH ₃	0.001	-0.002	2.544	-0.002	0.085	-0.073	2.052	0.011
CO	0.009	-0.003	3.018	0.005	0.012	-0.008	2.384	0.005
H ₂ CO	-0.029	0.090	2.128	0.063	0.043	-0.008	2.093	0.035
NH ₃	-0.074	0.128	2.561	0.054	0.059	-0.014	1.799	0.046
H ₂ O	-0.058	0.182	2.795	0.125	0.063	-0.015	2.068	0.049
PH ₃	-0.017	0.016	2.144	0.000	0.000	0.003	1.714	0.003
H ₂ S	-0.025	0.028	2.245	0.003	0.013	0.001	1.834	0.009
CH ₃ ⁺	0.024	0.006	2.926	0.029	0.165	-0.115	2.427	0.049
NH ₄ ⁺	-0.046	0.063	2.763	0.018	0.032	-0.004	1.733	0.028
CN ⁻	-0.109	0.065	2.487	-0.043	0.029	-0.019	2.117	0.014
NH ₂ ⁻	-0.080	0.287	2.256	0.204	-0.007	0.038	1.913	0.030
OH ⁻	-0.034	0.251	2.650	0.218	0.038	0.029	2.346	0.065
SH ⁻	0.008	0.011	2.093	0.019	0.019	0.011	1.853	0.027
Br ⁻	0.016	-0.005	2.324	0.011	0.003	0.000	1.706	0.003
Cl ⁻	0.026	-0.011	2.378	0.017	0.006	0.005	1.780	0.008
F ⁻	0.023	-0.014	3.709	0.008	0.002	0.000	2.691	0.003

**Figure 2.** Change in the “rigid” part, $\Delta\eta^{f-}$, vs the change in the relaxation part, $\Delta\eta^{U-}$, of the electrophilic hardness upon solvation. Molecules above the dotted line show a decreasing electrophilic hardness in solvent ($\Delta\eta^- < 0$) (all values in electronvolts).

a positive change in the hardness when passing from the gas phase to solution.

Because in the Coulomb integrals there is no direct contribution from the \mathbf{V} matrix, as opposed to the orbital energies, we do not observe a substantial change in the hardness between the gas phase and solvent, except for the molecules which significantly change their geometry. In Figure 2, we have shown the components of the electrophile hardness. In general, changes in the $\Delta\eta^{U-}$ case are more important than in $\Delta\eta^{f-}$, illustrating the role of relaxation; neglecting this effect may lead to wrong hardness sequences.

For LiF, LiH, NaF, and NaH, we observe a large change in the electrophilic hardness. It is interesting that in the gas phase we have similar values for molecules with the same metal

**Figure 3.** Change in the rigid part, $\Delta\eta^{f+}$, vs the change in the relaxation part, $\Delta\eta^{U+}$, of the nucleophilic hardness upon solvation. Molecules below the dotted line show a decreasing nucleophilic hardness in solvent ($\Delta\eta^+ < 0$) (all values in electronvolts).

(~ 2.65 eV for LiF and LiH, ~ 2.45 eV for NaF and NaH), but in solvent, none of the metal makes the difference: $\eta_{\text{LiF}} \approx \eta_{\text{NaF}}$ and $\eta_{\text{LiH}} \approx \eta_{\text{NaH}}$. The hydrogen bond formed by the fluorine atom is stronger than the bond formed between hydrogen and a water oxygen. According to this, we observe large changes in the relaxation part of the electrophilic hardness for LiF and NaF. The order from the gas phase is preserved. HF is harder than HCl, H₂O than H₂S, NH₃ than PH₃, and OH⁻ than SH⁻.

The changes in nucleophilic hardness are quite small. We observe decreasing hardness only for those molecules which show significant changes in geometry (Figure 3), essentially due to the relaxation effect.

It is interesting to note that both in the orbital energy difference and the perturbational approach, the hardness in most

TABLE 3: Calculated Values for Atomic Mulliken Populations (q^{Mull} in arbitrary units) and Atomic Softness (in 10 per electronvolt)

molecule	atom	q^{Mull}		s^-		s^+		s^A		s^O	
		gas	solvent	gas	solvent	gas	solvent	gas	solvent	gas	solvent
LiF	F	9.66	9.79	1.175	1.210	0.073	-0.053	0.624	0.578	0.775	0.850
	Li	2.34	2.21	0.711	0.405	3.234	4.115	1.973	2.260	1.627	1.461
LiH	H	1.18	1.82	0.547	1.155	0.352	0.124	0.450	0.639	0.477	0.866
	Li	2.82	2.18	1.346	0.406	3.035	3.879	2.191	2.142	1.952	1.380
NaF	F	9.70	9.83	1.241	1.249	0.103	0.019	0.672	0.634	0.862	0.944
	Na	10.30	10.17	0.737	0.348	3.856	4.835	2.297	2.592	1.776	1.459
NaH	H	1.26	1.88	0.624	1.245	0.387	0.119	0.506	0.682	0.544	0.959
	Na	10.74	10.12	1.499	0.307	3.735	4.456	2.617	2.381	2.259	1.358
HF	F	9.52	9.62	1.125	1.168	0.041	0.055	0.583	0.612	0.661	0.695
	H	0.48	0.38	0.319	0.236	1.891	1.845	1.105	1.040	0.992	0.920
HCl	Cl	17.24	17.39	1.691	1.757	0.658	0.621	1.175	1.189	1.212	1.226
	H	0.76	0.62	0.312	0.233	1.659	1.646	0.986	0.940	0.936	0.893
HCN	C	5.85	5.94	1.104	1.070	1.598	1.575	1.351	1.323	1.324	1.297
	H	0.57	0.42	0.237	0.167	0.256	0.170	0.247	0.169	0.246	0.168
	N	7.58	7.64	0.512	0.637	0.452	0.557	0.482	0.597	0.485	0.601
BeH ₂	Be	3.83	2.99	1.042	0.431	2.595	2.586	1.818	1.509	1.683	1.317
	H	1.09	1.51	0.473	0.804	0.116	0.170	0.295	0.487	0.326	0.544
BH ₃	B	4.88	4.73	0.151	0.083	1.460	1.345	0.806	0.714	0.736	0.648
	H	1.04	0.19	0.606	0.625	0.327	0.359	0.466	0.492	0.481	0.506
CO	C	5.73	5.71	1.175	1.159	1.618	1.607	1.396	1.383	1.370	1.357
	O	8.27	8.29	0.482	0.495	0.480	0.488	0.481	0.491	0.481	0.492
H ₂ CO	C	5.87	5.81	0.115	0.119	0.858	0.912	0.487	0.515	0.483	0.510
	H	0.86	0.82	0.665	0.612	0.416	0.393	0.540	0.502	0.541	0.504
	O	8.42	8.55	0.907	0.939	0.703	0.651	0.805	0.795	0.806	0.797
NH ₃	H	0.67	0.60	0.394	0.344	1.268	1.202	0.831	0.773	0.755	0.699
	N	8.00	8.19	0.767	0.881	-1.026	-0.895	-0.129	-0.007	0.028	0.147
H ₂ O	H	0.57	0.48	0.361	0.276	1.429	1.356	0.895	0.816	0.816	0.730
	O	8.87	9.04	1.067	1.162	-0.440	-0.352	0.313	0.405	0.426	0.525
PH ₃	H	1.01	1.00	0.387	0.378	0.399	0.393	0.393	0.385	0.392	0.384
	P	14.96	15.01	1.167	1.200	1.720	1.729	1.444	1.465	1.413	1.435
H ₂ S	H	0.89	0.83	0.305	0.276	0.640	0.641	0.473	0.458	0.456	0.441
	S	16.22	16.35	1.617	1.673	1.444	1.422	1.531	1.547	1.539	1.560
CH ₃ ⁺	C	6.07	6.03	0.473	0.492	1.186	1.140	0.830	0.816	0.797	0.788
	H	0.64	0.66	0.412	0.399	0.290	0.293	0.351	0.346	0.357	0.351
NH ₄ ⁺	H	0.51	0.47	0.326	0.288	1.047	0.999	0.686	0.643	0.604	0.564
	N	7.95	8.13	0.507	0.649	-1.307	-1.153	-0.400	-0.252	-0.192	-0.050
	C	6.35	6.20	1.257	1.183	1.571	1.554	1.414	1.369	1.401	1.356
CN ⁻	N	7.65	7.80	0.754	0.864	0.788	0.793	0.771	0.829	0.770	0.831
	N	8.58	8.21	1.306	0.900	-0.387	-0.270	0.460	0.315	0.529	0.384
NH ₂ ⁻	H	0.71	0.90	0.457	0.565	1.500	1.420	0.979	0.992	0.936	0.942
	H	0.79	0.61	0.621	0.382	1.884	1.999	1.252	1.190	1.213	1.120
OH ⁻	O	9.21	9.40	1.266	1.362	0.250	0.075	0.758	0.718	0.789	0.774
	H	1.03	0.90	0.330	0.279	1.281	1.338	0.805	0.809	0.776	0.778
SH ⁻	S	16.97	17.10	2.060	2.089	1.422	1.322	1.741	1.705	1.761	1.728
	Br	36.00	36.00	2.152	2.142	2.931	2.926	2.542	2.534	2.482	2.473
Cl ⁻	Cl	18.00	18.00	2.101	2.088	2.814	2.796	2.457	2.442	2.406	2.391
	F ⁻	F	10.00	10.00	1.349	1.346	1.857	1.856	1.603	1.601	1.563

cases increases, in agreement with Pearson's results³⁸ but opposed to the results obtained with the continuum model in⁴¹ which in view of the analytical expression derived are always negative. A hardness increase on the other hand was found invariably by Pérez et al.¹⁷ A difference in sign between $\Delta\eta^{\text{f}\pm}$ and $\Delta\eta^{\text{U}\pm}$ as obtained in some cases in Table 2 may play an important role; absolute values of both terms are mostly smaller than in the two aforementioned papers.^{17,41}

IV.2. Effect of Solvent on Condensed Properties Such as the Fukui Function and Local Softness. In Table 3, we report the atomic softness values. The atomic softness is the product of the condensed Fukui function and the global softness, the inverse of the global hardness, thereby combining local (atomic) and global information for a molecule. The analysis of the change in the frontier orbitals (HOMO and LUMO) has shown that using the EFP method, we do not observe an influence of the solvent on the rigid part of the condensed FF. But the crucial role of the hydrogen bond in the interactions between a molecule or ion and a solvent like water is manifested by a significant change in the relaxation part of the condensed FF.

The hardness or softness measures the resistance to change of the electron cloud, either by gain or loss of electrons or by

polarization. The electrophilic softness (system loses electrons) measures the reactivity toward an electrophilic reagent and affords a comparison between the donor atoms or molecules such as Lewis bases. When the system gains electrons, we use the nucleophilic softness (measures reactivity toward a nucleophilic reagent) for the Lewis acids, which are electron acceptors. The atomic softness increases for donor atoms in such bases, e.g., the nitrogen atom in NH₃ and HCN, the oxygen atom in H₂O, H₂CO, and CO, or the halides in protic acids such as HF and HCl or salts such as NaF and LiF. For molecules which change their geometry, the increase in electrophilic softness is larger than for the rest of the molecules. The hydrogen atoms in LiH, NaH, and BeH₂ are softer in the solvent than in the gas phase. Analogous trends are observed for the fluorine atoms in NaF and LiF. The influence of the solvent on the atomic softness for Lewis acids is not clear. For H⁺, we observe a decreasing nucleophilic softness in protic acids, e.g., HCl, HF, and HCN. For Na⁺ and Li⁺, the atomic softness however increases for the reaction toward nucleophilic reagents. The acid character of these cations is clearer in the solvent phase than in the gas phase. For the beryllium atom in BeH₂, we observe only a

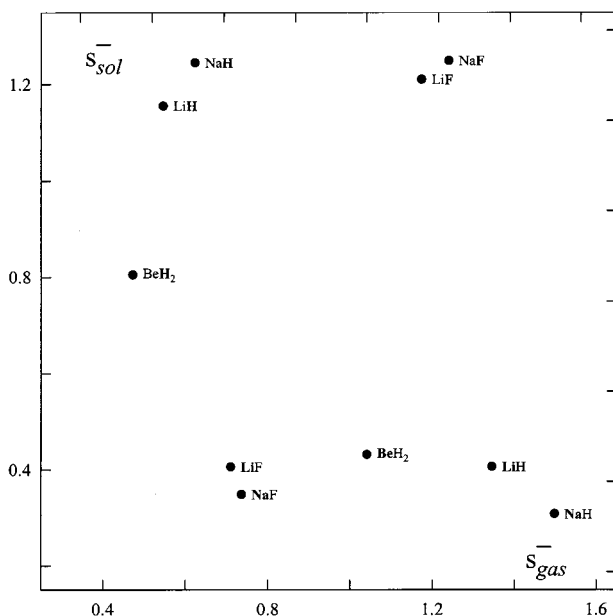


Figure 4. Electrophilic atomic softness in the gas phase, S_{gas}^- vs the atomic softness in solvent for atoms (bold) in molecules, S_{sol}^- with a significant change in the binding function (all values in 10 per electronvolt).

decreasing electrophilic softness; paradoxically, the nucleophilic softness does not change.

These results can be considered as the specific interaction counterpart of the continuum model-based studies on the evolution of the Fukui function (and its derivatives) upon solvation, for example, on the enolate ion.^{20,43}

In Figure 4, we have shown the change in the atomic softness values for those molecules, which show a considerable change in their geometry during solvation. The fluorine anion is seen to change its electrophilic softness upon solvation. The softness of H^- resides in its ability to donate charge to an acid for σ -bonding; due to solvation, the charge on the hydrogen atom increases, and we also observe an increase in the electrophilic softness in water. During solvation, the internuclear distance increases for this group of molecules and the charge separation between Na and Li, and H and F, increases. As a result of this, the differences between the softness values for lithium and sodium cation compounds with F^- and H^- in the gas phase disappear upon solvation. The values, which for these cations are very close, prove that in these cases we have very well separated ion pairs.

V. Conclusion

The effective fragment potential (EFP) model has been used to study the effect of adding 30 water molecules on several DFT-based reactivity descriptors of some neutral molecules, molecular ions, and anions. The binding function for the solvated geometry in the gas phase nicely monitors the solvation of the molecule. Values of the binding function for LiF, LiH, NaF, NaH, and BeH_2 are 1 order of magnitude larger than for the other species. We do not observe a decreasing HOMO–LUMO gap in the solvent. All anions exhibit a significant change in the chemical potential. Both HOMO and LUMO energy levels decrease in the solvent phase versus the gas phase. For the major part of the acids, the increase in the LUMO energy is larger than in the HOMO energy. For the group of salts, we observe an increase in the LUMO energy level and a resulting similar decrease in the HOMO energy level; the solvent effect was

shown when analyzing the hardness and condensed Fukui function. For LiF, LiH, NaF, and NaH, we observe a large change in the electrophilic hardness. The atomic softness increases for donor atoms in bases such as the nitrogen atom in NH_3 and HCN, the oxygen atom in H_2O , H_2CO , and CO, or the halogen atom in the protic acids HX (HF and HCl) or in salts such as NaF and LiF. For molecules, which change their geometry, increasing the electrophilic softness is larger than for the rest of the molecules. The influence of the solvent on the atomic softness of acceptor atoms in Lewis acids is not clear. We observe both trends, increasing and decreasing atomic softness. Very close values for the same ions in molecules such as LiH, LiF, NaH, NaF, and LiF indicate that in these cases we have very good separated ion pairs. Analysis of the values for the other molecules suggests that for a good description of the solvent effect on the reactivity indices in future we should use at least one molecule of water which will be treated in the same way as the solute molecule within the EFP context.

Acknowledgment. P.G. acknowledges the Free University of Brussels (VUB) for a generous computer grant and the Fund for Scientific Research-Flanders (FWO) for continuous support. B.S. thanks the “Fondation Van Buuren” for financial support. R.B. acknowledges NATO for a research fellowship. The work was supported by a research grant from the Flemish Polish Scientific Cooperation Program.

References and Notes

- Parr, R. G.; Yang, W. *Density Functional Theory of Atoms and Molecules*; Oxford University Press: New York, 1998.
- Koch, W.; Holthausen, M. C. *A Chemist's Guide to Density Functional Theory*; VCM: Weinheim, Germany, 2000.
- Parr, R. G.; Donnelly, R. A.; Levy, M.; Palke, W. E. *J. Chem. Phys.* **1978**, *68*, 3801.
- Parr, R. G.; Pearson, R. G. *J. Am. Chem. Soc.* **1983**, *105*, 7512.
- Berkowitz, M.; Parr, R. G. *J. Chem. Phys.* **1988**, *88*, 2554.
- Yang, W.; Parr, R. G. *Proc. Natl. Acad. Sci. U.S.A.* **1984**, *82*, 6723.
- Parr, R. G.; Yang, W. *J. Am. Chem. Soc.* **1984**, *106*, 4049.
- Li, Y.; Evans, N. S. *J. Am. Chem. Soc.* **1995**, *117*, 7756.
- Sanderson, R. T. *J. Am. Chem. Soc.* **1952**, *74*, 272; *Science* **1951**, *114*, 670.
- Pearson, R. G. *J. Chem. Educ.* **1987**, *64*, 561.
- Geerlings, P.; De Proft, F.; Langenaeker, W. *Adv. Quantum Chem.* **1999**, *33*, 303.
- Geerlings, P.; De Proft, F.; Martin, J. L. M. *Theor. Comput. Chem.* **1996**, *4*, 773.
- De Proft, F.; Geerlings, P. *Chem. Rev.* **2001**, *101*, 1451.
- Chermette, H. *J. Comput. Chem.* **1999**, *20*, 128.
- Safi, B.; Choho, K.; De Proft, F.; Geerlings, P. *Chem. Phys. Lett.* **1999**, *300*, 85.
- Safi, B.; Choho, K.; De Proft, F.; Geerlings, P. *J. Phys. Chem. A* **1998**, *102*, 5253.
- Pérez, P.; Contreras, R.; Aizman, A. *THEOCHEM* **1997**, *390*, 169.
- Pérez, P.; Contreras, R.; Aizman, A. *Chem. Phys. Lett.* **1996**, *260*, 236.
- Contreras, R.; Safont, V. S.; Pérez, P.; Andrés, J.; Moliner, V.; Tapia, O. *THEOCHEM* **1998**, *426*, 277.
- Contreras, R.; Domingo, L. R.; Andrés, J.; Pérez, P.; Tapia, O. *J. Phys. Chem. A* **1999**, *103*, 1367.
- Balawender, R.; Safi, B.; Geerlings, P. *J. Phys. Chem. A* **2001**, *105*, 6703.
- Day, P. N.; Jensen, J. H.; Gordon, M. S.; Webb, P.; Stevens, W. J.; Krauss, M.; Garmer, D. R.; Basch, H.; Cohen, D. *J. Chem. Phys.* **1996**, *105*, 1968.
- Freitag, M. A.; Gordon, M. S.; Jensen, J. H.; Stevens, W. J. *J. Chem. Phys.* **2000**, *112*, 7300.
- Wladkowski, B. D.; Krauss, M.; Stevens, W. J. *J. Am. Chem. Soc.* **1995**, *117*, 10537.
- Merrill, G. N.; Gordon, M. S. *J. Phys. Chem. A* **1998**, *102*, 2650.
- Chen, W.; Gordon, M. S. *J. Chem. Phys.* **1996**, *105*, 11081.
- Krauss, M.; Webb, S. P. *J. Chem. Phys.* **1997**, *107*, 5771.
- Day, P. N.; Pachter, R. *J. Chem. Phys.* **1997**, *107*, 2990.
- Peterson, C. P.; Gordon, M. S. *J. Phys. Chem. A* **1999**, *103*, 4166.
- Bandyopadhyay, P.; Gordon, M. S. *J. Chem. Phys.* **2000**, *113*, 1104.
- Balawender, R.; Komorowski, L. *J. Chem. Phys.* **1998**, *109*, 5203.

- (32) Balawender, R.; Geerlings, P. *J. Chem. Phys.* **2001**, *114*, 682.
- (33) Wang, X.; Peng, Z. *Int. J. Quantum Chem.* **1993**, *47*, 393.
- (34) Balawender, R.; De Proft, F.; Geerlings, P. *J. Chem. Phys.* **2001**, *114*, 4441.
- (35) Schmidt, M. W.; Baldrige, K. K.; Boatz, J. A.; Elbert, S. T.; Gordon, M. S.; Jensen, J. J.; Koseki, S.; Matsunaga, N.; Nguyen, K. A.; Su, S.; Windus, T. L.; Dupuis, M.; Montgomery, J. A. *GAMESS. J. Comput. Chem.* **1993**, *14*, 1347.
- (36) Berry, R. S.; Rice, S. A.; Ross, J. *Physical Chemistry*, 2nd ed.; Oxford University Press: New York, 2000, and references therein.
- (37) Diercksen, G. H. F.; Karelson, M.; Tamm, T.; Zerner, M. C. *Int. J. Quantum Chem.* **1994**, *28*, 339 and references therein.
- (38) Pearson, G. *J. Am. Chem. Soc.* **1986**, *108*, 6109.
- (39) Pearson, R. G. *J. Chem. Educ.* **1968**, *45*, 581.
- (40) Pearson, R. G. *Inorg. Chim. Acta* **1995**, *240*, 93.
- (41) Pérez, P.; Toro-Labbé, A.; Contreras, R. *J. Am. Chem. Soc.* **2001**, *123*, 5527.
- (42) Jørgensen, C. K. *Inorg. Chem.* **1964**, *3*, 1201.
- (43) Damoun, S.; Van de Woude, G.; Méndez, F.; Geerlings, P. *J. Phys. Chem. A* **1999**, *103*, 7861.